Optimal Independence-Checking Coding For Secure Uplink Training in Large-Scale MISO-OFDM Systems

Dongyang Xu*†, Pinyi Ren*†, and James A. Ritcey‡
*School of Electronic and Information Engineering, Xi'an Jiaotong University, China
†Shaanxi Smart Networks and Ubiquitous Access Research Center, China.
‡Department of Electrical Engineering, University of Washington, USA.
E-mail: {*xudongyang@stu.xjtu.edu.cn, pyren@mail.xjtu.edu.cn, ritcey@ee.washington.edu* }

***Abstract*—Due to the *publicly-known deterministic* characteristic of pilot tones, pilot-aware attack, by jamming, nulling and spoofing pilot tones, can significantly paralyze the uplink channel training in large-scale MISO-OFDM systems. To solve this, we in this paper develop an independence-checking coding based (ICCB) uplink training architecture for one-ring scattering scenarios allowing for uniform linear arrays (ULA) deployment. Here, we not only insert randomized pilots on subcarriers for channel impulse response (CIR) estimation, but also diversify and encode subcarrier activation patterns (SAPs) to convey those pilots simultaneously. The coded SAPs, though interfered by arbitrary unknown SAPs in wireless environment, are qualified to be reliably identified and decoded into the original pilots by checking the hidden channel independence existing in subcarriers. Specifically, an independence-checking coding (ICC) theory is formulated to support the encoding/decoding process in this architecture. The optimal ICC code is further developed for guaranteeing a well-imposed estimation of CIR while maximizing the code rate. Based on this code, the identification error probability (IEP) is characterized to evaluate the reliability of this architecture. Interestingly, we discover the principle of IEP reduction by exploiting the array spatial correlation, and prove that zero-IEP, i.e., perfect reliability, can be guaranteed under continuously-distributed mean angle of arrival (AoA). Besides this, a novel closed form of IEP expression is derived in discretely-distributed case. Simulation results finally verify the effectiveness of the proposed architecture.**

***Index Terms*—Physical layer security, pilot-aware attack, OFDM, channel estimation, independence-checking coding.**

I. Introduction

Security paradigms in wireless communications has attracted increasing attention with the evolution of air interface technology towards the requirements of future 5G networks. In those envisioned scenarios, multiple existing technologies, such as orthogonal frequency-division multiplexing (OFDM), are closely integrated with novel innovative attempts, such as large-scale multiple-antenna technique or namely massive multiple-input, multiple-output (Massive MIMO) [1]. And the phenomenon accompanied by is that the imperishable characteristic of wireless channels, such as the open and shared nature, have always been rendering those air interface technologies vulnerable to growing security attacks, including the denial of service (DoS) attacks and tampering attacks, among others. As a major manner of DoS attack, jamming attacks, in a variety of behaviors out of control, have exhibited its astonishing destructive power on those existing [2] and emerging air interface techniques [3].

A very typical example is that OFDM systems under large-scale antenna arrays are very suspectable to the protocol-aware attack, a well-directed attack that can sense the specific protocols and intensify the effectiveness of attack by jamming a physical layer mechanism instead of data payload directly. As a typical protocol-aware attack, pilot-aware attack could hinder the regular channel training between legitimate transceiver pair. This is done, in theory, by jamming/nulling/spoofing the deterministic pilot tones which are known and shared on the time-frequency resource grid (TFRG) by all parties for channel acquisition [4]–[6]. That is to say, pilot-aware attack could embrace three flexible modes, i.e., pilot tone jamming (PTJ) attack [5], pilot tone nulling (PTN) attack [5] and pilot tone spoofing (PTS) attack [6]. As an example of PTS attack in narrow-band single-carrier systems, pilot contamination (PC) attack was first introduced and analysed by [7]. Following [7], many research have been investigated on the advantage of large-scale multi-antenna arrays on defending against PC attack [8]–[10]. However, those studies were limited to the attack detection by exploiting the physical layer information, such as auxiliary training or data sequences [8], [9] and some prior-known channel information [10].

The first attempt to resolve pilot aware attack was proposed for a conventional OFDM systems in [11], that is, transforming the PTN and PTS attack into PTJ attack by randomizing the locations and values of regular pilot tones on TFRG. Assuming the independent subcarriers, authors in [6] proposed a frequency-domain subcarrier (FS) channel estimation framework under the PTS attack by exploiting pilot randomization and independence component analysis (ICA). One key problem is that the practical subcarriers are not mutually independent in the scenarios with limited channel taps, and thus ICA does not apply in this case. What's most important is that the influence of SAPs on CIR estimation was not evaluated. Actually, when the so-called optimal code is adopted, its CIR estimation is extremely ill-imposed and unprecise.

This further motives us to provide a secure large-scale multi-antenna OFDM systems, with some necessary consideration, i.e., array spatial correlation, and redesign the overall pilot sharing process during the uplink channel training phase. Most importantly, we have to redesign the supporting CIR estimation process. Before that, we have to admit that the pilot randomization technique, though necessary for resolving pilot-aware attack, brings to the process two bottlenecks, i.e., unpredictable attack modes and non-recoverable pilot information covered by random wireless channels. Basically, an efficient hybrid attack is more likely to be the following:

Problem 1 (**Attack Model**). *An attacker in hybrid attack mode can choose either PTJ mode or silence cheating (SC) mode for intentional information hiding as well.*

Two notes should be noticed, that is, 1) an attacker in PTJ mode could choose two behaviors, i. e., wide-band pilot jamming (WB-PJ) attack and partial-band pilot jamming (PB-PJ) attack. 2) the attacker in SC mode turns to keep silent for cheating the legitimate node. In this case, though the legitimate node adopts random pilots by supposing the attacker exists, the attacker actually does not pay the price since it does not jam at all.

On the other hand, we could further identify the second bottleneck as follows:

Problem 2. *Randomized pilots, if utilized for uplink channel training through wireless channels, cannot be separated, let alone identified.*

This issue refers to three fundamental concepts which are respectively recognized as pilot conveying, separation and identification in this paper. Here, the innovative methodology we introduce is: *Selectively activate and deactivate the OFDM subcar- riers and create various SAP candidates. Diversify SAPs to encode pilots and reuse those coded subcarriers carrying pilot information, to estimate the uplink channels simultaneously.* In what follows, the main contributions of this paper are summarized:

1) First, a deterministic and precise encoding principle is established such that arbitrary SAPs can be encoded as a binary code. The ICC theory is then developed to further optimize the code such that arbitrary two codewords in the code, if being superimposed on each other, can be separated and identified reliably. Furthermore, an optimal ICC codebook is formulated with the maximum code rate while guaranteeing a well-imposed CIR estimation. Based on this code, a reliable ICCB uplink training architecture is finally built up by constructing an one-to-one mapping/demapping relationship between pilots, codewords and SAPs.
2) We further characterize the reliability of this architecture as the identification error probability (IEP) and discover a hidden phenomenon that when subcarrier estimations are performed on the basis of this architecture, the array spatial correlation existing in the subcarriers overlapped from the legitimate node and the attacker can further reduce IEP. At this point, the attacker can actually help the legitimate node to improve the reliability. Interestingly, it can also be proved that zero IEP cannot be achieved only when the attacker is located in the clusters with the same mean AoA as the legitimate node. This principle, in theory, could facilitate the acquisition of the position of Ava. If we consider the mean AoA with continuous distribution, the reliability, in this sense, can be perfectly guaranteed. Otherwise, for a practical discrete distribution model, we again show how much the reliability could be further reinforced.

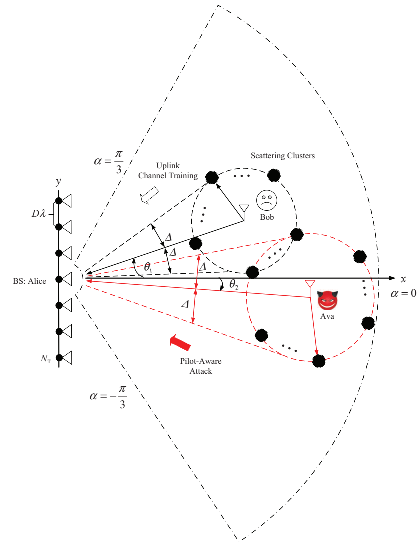

Fig. 1. Diagram of large-scale MISO-OFDM system under the wide-band one-ring scattering model. In this system, AoA ranges of Bob and Ava overlap, which incurs an effective pilot-aware attack on the uplink channel estimation.

The rest of the paper is summarized as follows. In section II, we present an overview of pilot-aware attack on multi-antenna OFDM systems. In Section III, we introduce an ICCB uplink training architecture. Channel estimation and identification enhancement is described in Section IV. Numerical results are presented in Section V and finally we conclude our work in Section VI.

II. Overview of Pilot-Aware Attack on Multi-Antenna OFDM Systems

In this section, we will provide a basic overview of pilot-aware attack by introducing three basic configurations, including the system and signal model as well as the channel estimation model. Under this background, we will then review the influence of a common-sense technique, i.e., pilot randomization, on the pilot-aware attack and identify the existing key impediments.

A. System Description

We consider an synchronous large-scale MISO-OFDM system with a $N_{\mathrm{T}} \gg 1$-antenna base station (named as Alice) and a single-antenna legitimate user (named as Bob). As shown in Fig. 1, the based station (BS) with angle spread Δ is equipped with a $D\lambda$-spacing directive ULA and placed at the origin along the y-axis to serve a 120-degree sector that is centered around the x-axis ($\alpha = 0$). We assume that no energy is received for angles $\alpha \notin \left[-\frac{\pi}{3}, \frac{\pi}{3}\right]$. Furthermore, we consider the wide-band one-ring scattering model for which Bob is surrounded by local scatterers within $[\theta_1 - \Delta, \theta_1 + \Delta]$ [12],

[13]. Here θ_1 represents the mean AoA of clusters surrounding Bob.

In this system, pilot-tone based uplink channel training process is considered in which N available subcarriers indexed by Ψ are provided during each available OFDM symbol time. In principle, $N_{\rm B}$ subcarriers indexed by $\Psi_{\rm B}=\{i_0, i_1, \ldots, i_{N_{\rm B}-1}\}$ are employed for pilot tone insertion and the following channel estimation. A single-antenna malicious node (named as Ava) then aims to disturb this training process by jamming/spoofing/nulling those pilot tones. We denote the set of victim subcarriers by $\Psi_{\rm A}=\{i_0, i_1, \ldots, i_{N_{\rm A}-1}\}$ where $N_{\rm A}$ denotes the number of victim subcarriers. Furthermore, we make the following assumption:

Assumption 1. *Ava is surrounded by local scatterers within* $[\theta_2-\Delta, \theta_2+\Delta]$ *and always has the overlapping AoA intervals with Bob, this is,* $[\theta_2-\Delta, \theta_2+\Delta] \cap [\theta_1-\Delta, \theta_1+\Delta] \neq \emptyset$. *Here,* θ_2 *denotes the mean AoA of clusters surrounding Ava.*

This assumption is supported by the scenario where a common large scattering body (e.g., a large building) could create a set of angles common to all nodes in the system and the overlapping is inevitable. The result is that the channel covariance eigenspaces of two nodes are coupled and the attack is hard to be eliminated through angular separation [12].

B. Receiving Signal Model

To begin with, we denote pilot tones of Bob and Ava at the j-th subcarrier and k-th symbol time, respectively by $x_{\rm B}^j[k], j \in \Psi_{\rm B}$ and $x_{\rm A}^j[k], j \in \Psi_{\rm A}$.

Assumption 2. *We in this paper assume* $x_{\rm B}^i[k] = x_{\rm B}[k] = \sqrt{\rho_{\rm B}} e^{j\phi_k}, i \in \Psi_{\rm B}$ *for low overhead consideration and theoretical analysis. Alternatively, we can superimpose* $x_{\rm B}[k]$ *onto a dedicated pilot sequence optimized under a non-security oriented scenario. At this point,* ϕ_k *can be an additional phase difference for security consideration. We do not constraint the strategies of pilot tones of Ava such that* $x_{\rm A}^i[k] = \sqrt{\rho_{\rm A}} e^{j\varphi_{k,i}}, i \in \Psi_{\rm A}$.

Let us proceed to the basic OFDM procedure. First, the frequency-domain pilot signals of Bob and Ava over N subcarriers are respectively stacked as N by 1 vectors $\mathbf{x}_{\rm B}[k] = [x_{{\rm B},j}[k]]_{j\in\Psi}^{\rm T}$ and $\mathbf{x}_{\rm A}[k] = [x_{{\rm A},j}[k]]_{j\in\Psi}^{\rm T}$. Here there exist:

$$x_{{\rm B},j}[k] = \left\{ \begin{array}{cc} x_{\rm B}[k] & j \in \Psi_{\rm B} \\ 0 & j \notin \Psi_{\rm B} \end{array} \right., x_{{\rm A},j}[k] = \left\{ \begin{array}{cc} x_{\rm A}^j[k] & j \in \Psi_{\rm A} \\ 0 & j \notin \Psi_{\rm A} \end{array} \right. \tag{1}$$

Assume that the length of cyclic prefix is larger than L. The parallel streams, i.e., $\mathbf{x}_{\rm B}[k]$ and $\mathbf{x}_{\rm A}[k]$, are modulated with inverse fast Fourier transform (IFFT). After removing the cyclic prefix at the i-th receive antenna and k-th OFDM symbol time, Alice derive the time-domain N by 1 vector $\mathbf{y}^i[k]$ as:

$$\mathbf{y}^i[k] = \mathbf{H}_{\rm C,B}^i \mathbf{F}^{\rm H} \mathbf{x}_{\rm B}[k] + \mathbf{H}_{\rm C,A}^i \mathbf{F}^{\rm H} \mathbf{x}_{\rm A}[k] + \mathbf{v}^i[k] \tag{2}$$

where $\mathbf{H}_{\rm C,B}^i$ and $\mathbf{H}_{\rm C,A}^i$ are $N \times N$ circulant matrices for which the first column of $\mathbf{H}_{\rm C,B}^i$ and $\mathbf{H}_{\rm C,A}^i$ are respectively given by $\left[\begin{array}{cc} \mathbf{h}_{\rm B}^{i\rm T} & \mathbf{0}_{1\times(N-L)} \end{array}\right]^{\rm T}$ and $\left[\begin{array}{cc} \mathbf{h}_{\rm A}^{i\rm T} & \mathbf{0}_{1\times(N-L)} \end{array}\right]^{\rm T}$. Here, $\mathbf{h}_{\rm B}^i \in \mathbb{C}^{L\times 1}$ and $\mathbf{h}_{\rm A}^i \in \mathbb{C}^{L\times 1}$ are CIR vectors, respectively from Bob and Ava to the i-th receive antenna of Alice. $\mathbf{h}_{\rm A}^i$ is assumed to be independent with $\mathbf{h}_{\rm B}^i$. $\mathbf{v}^i[k] \in \mathbb{C}^{N\times 1}$ with $\mathbf{v}^i[k] \sim \mathcal{CN}\left(0, \mathbf{I}_N \sigma^2\right)$ is the AWGN vector at the i-th antenna and k-th symbol time Taking FFT, Alice finally derives the frequency-domain N by 1 signal vector at the i-th receive antenna and k-th OFDM symbol time as

$$\tilde{\mathbf{y}}^i[k] = {\rm diag}\{\mathbf{x}_{\rm B}[k]\} \mathbf{F}_{\rm L} \mathbf{h}_{\rm B}^i + {\rm diag}\{\mathbf{x}_{\rm A}[k]\} \mathbf{F}_{\rm L} \mathbf{h}_{\rm A}^i + \mathbf{w}_N^i[k] \tag{3}$$

Here, there exists $\mathbf{F}_{\rm L} = \sqrt{N}\mathbf{F}(:, 1:L)$ where $\mathbf{F}$ denotes the DFT matrix. And we have $\mathbf{w}_j^i[k] = \mathbf{F}_j \mathbf{v}^i[k]$ where $\mathbf{F}_j$ is the j-row submatrix of $\mathbf{F}$. Throughout this paper, we assume that the CIRs belonging to different paths at each antenna exhibit spatially uncorrelated Rayleigh fading. We denote power delay profiles (PDPs) of the l-th path of Bob and Ava, respectively by $\sigma_{{\rm B},l}^2$, $\sigma_{{\rm A},l}^2$. Without loss of generality, each path has the uniform and normalized PDP satisfying $\sum\limits_{l=1}^{L} \sigma_{{\rm B},l}^2 = 1, \sum\limits_{l=1}^{L} \sigma_{{\rm A},l}^2 = 1$ [14]. For each path, CIRs of different antennas are assumed to be spatially correlated. In one-ring scattering scenarios, the correlation between the channel coefficients of antennas $1 \leq m, n \leq N_{\rm T}$, $\forall l$ can be defined by [12]:

$$[\mathbf{R}_k]_{m,n} = \frac{1}{2\Delta} \int_{-\Delta+\theta_k}^{\Delta+\theta_k} e^{-j2\pi D(m-n)\sin(\theta)} d\theta, k = 1, 2 \tag{4}$$

Here, $\mathbf{R}_i$ represents the channel covariance matrix of Bob if $i = 1$ and Ava otherwise. $\mathbf{R}_1$, instead of $\mathbf{R}_2$, is known by Alice.

C. Channel Estimation Model

Now let us turn to describe the estimation models of FS channels under specific attacks. First, Ava under PTS attack mode could learn the pilot tones employed by Bob in advance and impersonate Bob by utilizing the same pilot tone learned. In this case, there exists $\Psi_{\rm B} \cup \Psi_{\rm A} = \Psi_{\rm B}$ and $x_{\rm A}^i[k] = x_{\rm B}[k], i \in \Psi_{\rm B}$. Signals in Eq. (3) can be rewritten as:

$$\tilde{\mathbf{y}}_{\rm PTS}^i[k] = \mathbf{F}_{\rm L} \mathbf{h}_{\rm B}^i x_{\rm B}[k] + \mathbf{F}_{\rm L} \mathbf{h}_{\rm A}^i x_{\rm B}[k] + \mathbf{w}_N^i[k] \tag{5}$$

Finally, a least square (LS) based channel estimation is formulated by: $\widehat{\mathbf{h}}_{con}^i = \mathbf{h}_{\rm B}^i + \mathbf{h}_{\rm A}^i + (\mathbf{F}_{\rm L})^{+} \frac{x_{\rm B}^{\rm H}[k]}{\left|x_{\rm B}^{\rm H}[k]\right|^2} \mathbf{w}_N^i[k]$ where $(\mathbf{F}_{\rm L})^{+}$ is the MoorePenrose pseudo-inverse of $\mathbf{F}_{\rm L}$. We see that the estimation of $\mathbf{h}_{\rm B}^i$ is contaminated by $\mathbf{h}_{\rm A}^i$ with a noise bias when a PTS attack happens.

As to PTN attack, we emphasize the difference lying in the fact that there exists ${\rm diag}\{\mathbf{x}_{\rm A}[k]\} = \mathbf{\Sigma} \odot x_{\rm A}[k]$ such that $\mathbf{\Sigma} \mathbf{F}_{\rm L} \mathbf{h}_{\rm A}^i x_{\rm A}[k] = -\mathbf{F}_{\rm L} \mathbf{h}_{\rm B}^i x_{\rm B}[k]$. Obviously, Ava can derive a unique solution of the diagonal matrix $\mathbf{\Sigma}$ because the assumed Ava can get both $\mathbf{h}_{\rm B}^i$ and $\mathbf{h}_{\rm A}^i$ (a very strong assumption in [5]). In this case, the received signals can be rewritten as $\tilde{\mathbf{y}}_{\rm PTN}^i[k] = \mathbf{w}_N^i[k]$. We see that the received signals are completely random noises, which can be seen as the worst destruction.

In order to represent the case where PTJ attack happens, we configure the matrix $\mathbf{\Sigma}$ with random input values. The

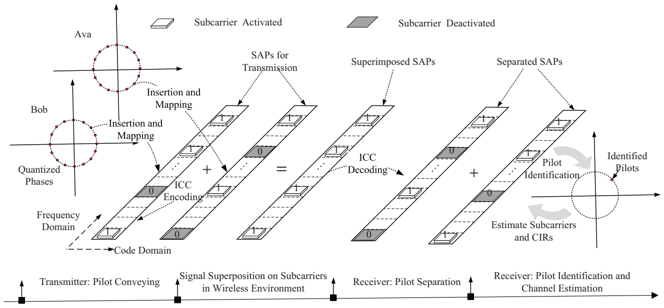

Fig. 2. Diagram of ICCB uplink channel training procedures.

estimated channels are with the similar form as those in PTS attack. The difference is that unlike PTS attack, the estimated channels cannot benefit both Bob and Ava, which is least efficient.

D. Influence of Pilot Randomization on Pilot-Aware Attack

To defend against pilot-aware attack, the commonsense is that Bob shall randomize its own pilot tones. In practice, the randomization of pilot tone values is employed. More specifically, each of the candidate pilot phases is mapped into a unique quantized samples, chosen from the set $\mathcal{A}$, defined by $\mathcal{C} = \{\phi : \phi = 2m\pi/C, 0 \le m \le C-1\}$ where C reflects the quantization resolution. This type of pilot randomization, due to the constraint of discrete phase samples, practically could not prevent a hybrid attack from happening but serves as a prerequisite for defending against pilot aware attack.

In what follows, we make the following assumption for Bob for the sake of theoretical analysis:

Assumption 3. *During two adjacent OFDM symbol time, such as, $k_i, k_{i+1}, i \ge 0$, two pilot phases ϕ_{k_i} and $\phi_{k_{i+1}}$ are kept with fixed phase difference, that is, $\phi_{k_{i+1}} - \phi_{k_i} = \overline{\phi}$. Here, $\phi_{k_{i+1}}$ and ϕ_{k_i} are both random but $\overline{\phi}$ are deterministic and publicly known.*

Institutively, how the value C increases affects the performance of anti-attack technique. However, things seem not to be simple as we think. As discussed in the Introduction part, a fact is that randomized pilots, if utilized for uplink channel training through wireless channels, cannot be separated, let alone identified.

III. ICCB Uplink Training Architecture

In view of above issues, we in this section aim to construct a novel pilot sharing mechanism, logically including three key procedures, i.e., pilot conveying, pilot separation and pilot identification. Each procedure can be found in Algorithm 1 and Fig. 2.

A. Pilot Conveying via Binary Code on Code-Frequency Domain

1) Binary Code: The Eq. (40) in [15] provides a decision threshold function $\gamma \triangleq f(N_{\mathrm{T}}, P_f)$, for measuring how many antennas on one subcarrier are required to achieve a certain probability P_f of false alarm. Here we consider three symbol time and a $3 \times N_{\mathrm{T}}$ receiving signal matrix is created for detection. Under this requirement, we try to build up a relationship between SAPs with the common binary code. Before that, we have the following definition:

Definition 1. *One subcarrier can be precisely encoded if, for any $\varepsilon > 0$, there exists a positive number $\gamma(\varepsilon)$ such that, for all $\gamma \ge \gamma(\varepsilon)$, P_f is smaller than ε.*

We should note that $f(N_{\mathrm{T}}, P_f)$ is a monotone decreasing function of two independent variables N_{T} and P_f. For a given probability constraint ε^*, we could always expect a lower bound $\gamma(\varepsilon^*)$ of possible thresholds such that $\gamma(\varepsilon^*) = f(N_{\mathrm{T}}, \varepsilon^*)$ is satisfied. Under this equation, we could flexibly configure N_{T} and $\gamma(\varepsilon^*)$ to make ε^* approach zero [15]. We also find that the γ that achieves zero-P_f is decreased with the increase of antennas. Basically, this phenomenon originates from the fact that the increased dimension makes the eigenvalues of noise matrix to be more concentrated in a narrow interval, which is determined by the well-known Marcenko-Pastur Law [16].

2) Code Frequency Domain: Based on Definition 1, we can encode the m-th subcarrier as a binary digit s_m according to:

$$s_m = \begin{cases} 1 & \text{if there exist signals} \\ 0 & otherwise \end{cases} \tag{6}$$

Meanwhile, let us denote a set of binary code vectors by $\mathcal{S}$ with $\mathcal{S} = \{\mathbf{s} | \, s_m \in \{0,1\}, 1 \le m \le L_s\}$ where L_s denotes the maximum length of the code. Then, a code frequency domain could be constructed as a set of pairs $(\mathbf{s}, b)$ with $\mathbf{s} \subset \mathcal{S}$ and $1 \le b \le N_{\mathrm{B}}$ where b is an integer representing the subcarrier index of appearance of the code. This can be depicted in Fig. 2.

3) Binary Codebook Matrix: On the formulated code-frequency domain, we group the binary digits and construct the binary code by presenting a binary codebook as follows:

Definition 2. *Given a $N_{\mathrm{B}} \times C$ binary matrix $\mathbf{C}$ with each element satisfying $c_{i,j} \in \mathbf{s} \subset \mathcal{S}$, we denote the i-th column of $\mathbf{C}$ by $\mathbf{c}_i$ with $\mathbf{c}_i = \begin{bmatrix} c_{1,i} & \cdots & c_{N_{\mathrm{B}},i} \end{bmatrix}^{\mathrm{T}}$. We call $\mathbf{C}$ a binary codebook matrix and $\mathbf{c}_i$ a codeword of $\mathbf{C}$ of length N_{B}.*

Based on this definition, we also define a superposition principle between codewords by the following:

Definition 3. *The superposition sum $\mathbf{z} = \mathbf{x} V \mathbf{y}$ (designated as the digit-by-digit Boolean sum) of two codewords denoted by $\mathbf{x} = (x_1, x_2, \ldots, x_{N_{\mathrm{B}}}) \subset \mathbf{C}$ and $\mathbf{y} = (y_1, y_2, \ldots, y_{N_{\mathrm{B}}}) \subset \mathbf{C}$ is defined by:*

$$z_i = \begin{cases} 0 & if \ x_i = y_i = 0 \\ 1 & otherwise \end{cases} \tag{7}$$

where z_i denotes the i-th element of vector $\mathbf{z}$.

Based on above preparations, the pilot conveying process can be shown in Algorithm 1.

B. Pilot Separation and Identification Via ICC

The study of how to optimize the previous binary codebook such that it can separate and identify codewords from the dis-

Algorithm 1 Pilot Conveying, Separation and Identification

1: **Pilot Conveying** 1) Insert one phase that is selected from set $\mathcal{A}$, onto subcarriers at the initial OFDM symbol, for instance defined by k_0. The phases of pilot signals inserted in adjacent OFDM symbols, such as $k_i, i \geq 1$ obey the Assumption 3.
2) Construct an one-to-one mapping from the phases in set $\mathcal{A}$ to codewords of binary codebook matrix derived in Section III-A, and then further to SAPs. Select one phase, i.e., the phase at k_0, for pattern activation. The specific principle is that pilot signals are transmitted on the i-th subcarrier if the i-th digit of the codeword is equal to 1, otherwise this subcarrier is kept unoccupied.

2: **Pilot Separation** Alice detects the available subcarriers to acquire the superimposed SAPs using the detection technique shown in [15]. Then Alice decodes those superimposed SAPs and derives two individual codewords by using the inner-product based differential decoding proposed in [6].

3: **Pilot Identification** Separated codewords that satisfy Theorem 1 are qualified to be identified and then demapped into the pilot phases in $\mathcal{A}$ for recovering the pilot signals of Bob.

turbed codeword is called ICC theory, including the encoding principle and decoding principle.

1) Encoding Principle: We introduce the concept of s-overlapping code with constant weight w by defining:

Definition 4. *A $N_{\mathrm{B}} \times C$ binary matrix $\mathbf{C}$ is called a ICC-(N_{B}, s) code of length N_{B} and order s, if for any column set $\mathcal{Q}$ such that $|\mathcal{Q}| = 2$, there exist at least a set $\mathcal{S}$ of s rows such that $c_{i,j} = 1, \forall i, j, i \in \mathcal{S}, j \in \mathcal{Q}$.*

In this principle, we can know that any two codewords in $\mathbf{C}$ must overlap with each other on at least s non-zero digits. Backing to the subcarriers, s means the overlapped subcarriers which are exploited for channel estimation. Now, we try to establish the relationship of s with the weight w of the code since the number of w determines the code rate.

Theorem 1. *The weight of ICC-(N_{B}, s) code of length N_{B} and order s satisfies $w = \frac{N_{\mathrm{B}}+s}{2}$ with $N_{\mathrm{B}} \geq s$. w is an integer smaller than N_{B}.*

Proof. See proof in Appendix VII-A. □

Here and in the following section, we assume the ratio of two integers is always kept to be an integer without loss of generality. Based on the theorem, we can derive the number of codewords or namely the columns in $\mathbf{C}$, by a binomial coefficient $C = \begin{pmatrix} N_{\mathrm{B}} \\ \frac{N_{\mathrm{B}}+s}{2} \end{pmatrix}$. Therefore, we have the following proposition:

Proposition 1. *The code rate of ICC-(N_{B}, s) code, defined by $R_{ICC} = \frac{\log_2(C)}{N_{\mathrm{B}}}$, is calculated as*

$$R_{ICC} = \log_2 \left[\frac{N_{\mathrm{B}}!}{\left(\frac{N_{\mathrm{B}}+s}{2}\right)! \left(\frac{N_{\mathrm{B}}-s}{2}\right)!} \right]^{1/N_{\mathrm{B}}} \tag{8}$$

Theorem 2. *The optimal ICC-(N_{B}, s) code maximizing the code rate holds when $s = L$. In this case, the reliability measured by IEP is given by*

$$P_{\mathrm{I}} = \frac{N_{\mathrm{B}}! - \left(\frac{N_{\mathrm{B}}+L}{2}\right)! \left(\frac{N_{\mathrm{B}}-L}{2}\right)!}{2^{N_{\mathrm{B}}+1} \left(\frac{N_{\mathrm{B}}+L}{2}\right)! \left(\frac{N_{\mathrm{B}}-L}{2}\right)!} \tag{9}$$

Proof. See proof in Appendix VII-B. □

2) Decoding Procedure: The related technique in this part is same with that in Fig. 3 of [6]. We do not specify this.

The overall process can be shown in Algorithm 1.

IV. Channel Estimation and Identification Enhancement

In this section, we continue our design work and focus on the channel estimation phase.

A. FS Channel Estimation

We do not consider the case where there is no attack since in this case LS estimator is a natural choice. If looking back to the pilot identification under a certain attack, we could derive two results, that is, one identified Bob's pilot vector or two confusing pilot vectors. For better considering the two cases, we in this section assume the identification error happens and forget the case without error, that is, we could get two confusing pilot vectors defined by $\mathbf{x}_{\mathrm{L},1} = \begin{bmatrix} x_{\mathrm{B}}[k_0] & x_{\mathrm{B}}[k_1] \end{bmatrix}^{\mathrm{T}}$ and $\mathbf{x}_{\mathrm{L},2} = \begin{bmatrix} x_{\mathrm{A}}[k_0] & x_{\mathrm{A}}[k_1] \end{bmatrix}^{\mathrm{T}}$ within two OFDM symbol time, i.e., k_0 and k_1. In this way, the estimator to be designed in this case can also apply in the another case naturally.

We consider two OFDM symbol time, i.e., k_0 and k_1 and $s, s \geq 1$ randomly-overlapping subcarriers. The randomness means their random positions of carrier frequency. Then the signals received on overlapping subcarriers within k_0 and k_1 are stacked as the $2 \times N_{\mathrm{T}}s$ matrix $\mathbf{Y}_{\mathrm{L}}$, equal to

$$\mathbf{Y}_{\mathrm{L}} = \mathbf{X}_{\mathrm{L}}\mathbf{H}_{\mathrm{L}} + \mathbf{N}_{\mathrm{L}} \tag{10}$$

where $\mathbf{X}_{\mathrm{L}}$ is denoted by a 2×2 matrix satisfying $\mathbf{X}_{\mathrm{L}} = \begin{bmatrix} \mathbf{x}_{\mathrm{L},1} & \mathbf{x}_{\mathrm{L},2} \end{bmatrix}$. The integrated $2 \times N_{\mathrm{T}}s$ channel matrix $\mathbf{H}_{\mathrm{L}}$ satisfies $\mathbf{H}_{\mathrm{L}} = \begin{bmatrix} \mathbf{h}_{\mathrm{B,L}}^{\mathrm{T}} & \mathbf{h}_{\mathrm{A,L}}^{\mathrm{T}} \end{bmatrix}^{\mathrm{T}}$. Here, there exist $\mathbf{h}_{\mathrm{B,L}} = \begin{bmatrix} \left(\mathbf{F}_{\mathrm{L},s}\mathbf{h}_{\mathrm{B}}^{i}\right)^{\mathrm{T}} & ,\ldots, & \left(\mathbf{F}_{\mathrm{L},s}\mathbf{h}_{\mathrm{B}}^{N_{\mathrm{T}}}\right)^{\mathrm{T}} \end{bmatrix}$ and $\mathbf{h}_{\mathrm{A,L}} = \begin{bmatrix} \left(\mathbf{F}_{\mathrm{L},s}\mathbf{h}_{\mathrm{A}}^{i}\right)^{\mathrm{T}} & ,\ldots, & \left(\mathbf{F}_{\mathrm{L},s}\mathbf{h}_{\mathrm{A}}^{N_{\mathrm{T}}}\right)^{\mathrm{T}} \end{bmatrix}$. $\mathbf{F}_{\mathrm{L},s}$ is the s-row matrix for which each index of s rows belongs to the set $\mathcal{P}_s$ that is defined by $\mathcal{P}_s = \{j_1, \ldots, j_s\}$, $\mathcal{P}_s \subseteq \Psi, |\mathcal{P}_s| = s$. $\mathbf{N}_{\mathrm{L}}$ represents the $2 \times N_{\mathrm{T}}s$ noise matrix with $\mathbf{N}_{\mathrm{L}} = \begin{bmatrix} \mathbf{w}_{\mathrm{L}}^{\mathrm{T}}[k_0] & \mathbf{w}_{\mathrm{L}}^{\mathrm{T}}[k_1] \end{bmatrix}^{\mathrm{T}}$ where there exists $\mathbf{w}_{\mathrm{L}}[k] = \begin{bmatrix} \mathbf{w}_s^{1^{\mathrm{T}}}[k] & ,\ldots, & \mathbf{w}_s^{N_{\mathrm{T}}^{\mathrm{T}}}[k] \end{bmatrix}$ for $k = k_0, k_1$.

Now we turn to the procedure of channel estimation. First, $\mathbf{x}_{\mathrm{L},1}$ and $\mathbf{x}_{\mathrm{L},2}$, are deemed as the candidate weight vectors for estimating. We then consider the sample covariance matrix given by $\mathbf{C}_{\mathbf{Y}_{\mathrm{L}}} = \frac{1}{N_{\mathrm{T}}s}\mathbf{Y}_{\mathrm{L}}\mathbf{Y}_{\mathrm{L}}^{\mathrm{H}}$ and finally derive the asymptotically-optimal linear minimum mean square error (LMMSE) estimators as $\mathbf{W}_{\mathrm{B,L}} = T_{\mathrm{B}}\mathbf{x}_{\mathrm{L},1}^{\mathrm{H}}\mathbf{C}_{\mathbf{Y}_{\mathrm{L}}}^{-1}$ and $\mathbf{W}_{\mathrm{A,L}} = T_{\mathrm{A}}\mathbf{x}_{\mathrm{L},2}^{\mathrm{H}}\mathbf{C}_{\mathbf{Y}_{\mathrm{L}}}^{-1}$, where $T_{\mathrm{B}} \triangleq \frac{\mathrm{Tr}(\mathbf{R}_{\mathrm{B,L}})\mathrm{Tr}(\mathbf{R}_{\mathrm{F}})}{N_{\mathrm{T}}s}$ and $T_{\mathrm{A}} \triangleq$

$\frac{\mathrm{Tr}(\mathbf{R}_{\mathrm{A,L}})\mathrm{Tr}(\mathbf{R}_{\mathrm{F}})}{N_{\mathrm{T}}q}$. Here, there exists $\mathrm{Tr}\left(\mathbf{R}_{\mathrm{B,L}}\right) = \mathrm{Tr}\left(\mathbf{R}_{\mathrm{A,L}}\right) = N_{\mathrm{T}}$ and therefore we could define $T_{\mathrm{B}} = T_{\mathrm{A}} = T$.

The estimated versions of FS channels are respectively derived as

$$\widehat{\mathbf{h}}_{\mathrm{B,L}}{=}\mathbf{W}_{\mathrm{B,L}}\mathbf{Y}_{\mathrm{L}}, \widehat{\mathbf{h}}_{\mathrm{A,L}}{=}\mathbf{W}_{\mathrm{A,L}}\mathbf{Y}_{\mathrm{L}} \tag{11}$$

The normalized mean square error (NMSE) for the two estimations are respectively defined by $\varepsilon_{\mathrm{B}}^2 = \frac{\mathbb{E}\left\{\left\|\widehat{\mathbf{h}}_{\mathrm{B,L}}-\mathbf{h}_{\mathrm{B,L}}\right\|^2\right\}}{N_{\mathrm{T}}s}, \varepsilon_{\mathrm{A}}^2 = \frac{\mathbb{E}\left\{\left\|\widehat{\mathbf{h}}_{\mathrm{A,L}}-\mathbf{h}_{\mathrm{A,L}}\right\|^2\right\}}{N_{\mathrm{T}}s}$ Furthermore, the relationship between the ideal channels with estimated versions can be given by $\mathbf{h}_{\mathrm{B,L}} = \widehat{\mathbf{h}}_{\mathrm{B,L}} + \varepsilon_{\mathrm{B}}\mathbf{h}$ and $\mathbf{h}_{\mathrm{A,L}} = \widehat{\mathbf{h}}_{\mathrm{A,L}} + \varepsilon_{\mathrm{A}}\mathbf{h}^{'}$ where $\varepsilon_{\mathrm{B}}\mathbf{h}$ is uncorrelated with $\mathbf{h}_{\mathrm{B,L}}$ and $\varepsilon_{\mathrm{A}}\mathbf{h}^{'}$ is uncorrelated with $\mathbf{h}_{\mathrm{A,L}}$. Here, the entries of $\mathbf{h}$ and $\mathbf{h}^{'}$ are i.i.d zero-mean complex Gaussian vectors with each element having unity variance.

Based on above results, we could have the following proposition:

Proposition 2. *With the large-scale antenna array, there exists $\varepsilon_{\mathrm{B}}^2 = \varepsilon_{\mathrm{A}}^2$ at high SNR .*

Proof: See proof in Appendix VII-C ∎

B. Identification Enhancement

Identification enhancement in this section means reducing IEP further. Since Bob could get two confusing pilots and two confusing estimated channels, we model the process of identification enhancement as a decision between two hypothesis:

$$\mathcal{H}_0 : \widehat{\mathbf{h}}_{\mathrm{B,L}} \rightarrow Bob, \mathcal{H}_1 : \widehat{\mathbf{h}}_{\mathrm{A,L}} \rightarrow Bob \tag{12}$$

For the sake of simplicity, we define the following eigenvalue decomposition:

$$\mathbf{R}_i = \mathbf{U}_i\mathbf{\Lambda}_i\mathbf{U}_i^{\mathrm{H}}, \mathbf{\Lambda}_i = diag\left\{\begin{array}{cccccc} \lambda_{i,1} & \cdots & \lambda_{i,\rho_i} & 0 & \cdots & 0 \end{array}\right\} \tag{13}$$

$$\overline{\mathbf{R}}_i = \mathbf{U}_i\overline{\mathbf{\Lambda}}_i\mathbf{U}_i^{\mathrm{H}}, \overline{\mathbf{\Lambda}}_i = diag\left\{\begin{array}{cccccc} \lambda_{i,1}^{-1} & \cdots & \lambda_{i,\rho_i}^{-1} & 0 & \cdots & 0 \end{array}\right\} \tag{14}$$

$$\mathbf{R}_{\mathrm{F}} = \mathbf{V}_{\mathrm{f}}\mathbf{\Sigma}_{\mathrm{f}}\mathbf{V}_{\mathrm{f}}^{\mathrm{H}}, \mathbf{\Sigma}_{\mathrm{f}} = diag\left\{\begin{array}{cccccc} \lambda_{\mathrm{f},1} & \cdots & \lambda_{\mathrm{f},\rho_{\mathrm{f}}} & 0 & \cdots & 0 \end{array}\right\} \tag{15}$$

$$\overline{\mathbf{R}}_{\mathrm{F}} = \mathbf{V}_{\mathrm{f}}\overline{\mathbf{\Sigma}}_{\mathrm{f}}\mathbf{V}_{\mathrm{f}}^{\mathrm{H}}, \overline{\mathbf{\Sigma}}_{\mathrm{f}} = diag\left\{\begin{array}{cccccc} \lambda_{\mathrm{f},1}^{-1} & \cdots & \lambda_{\mathrm{f},\rho_{\mathrm{f}}}^{-1} & 0 & \cdots & 0 \end{array}\right\} \tag{16}$$

where there exists $\mathbf{R}_{\mathrm{F}}{=}\mathbf{F}_{\mathrm{L},s}^{\mathrm{T}}\mathbf{F}_{\mathrm{L},s}^{*}$. The rank of $\mathbf{R}_i$ and $\mathbf{R}_{\mathrm{F}}$ are respectively denoted by ρ_i and $\rho_{\mathrm{f}} = \min\left\{s, L\right\}$. To identify the two hypothesis, we build up the error decision function as

$$\Delta f \triangleq f\left(\widehat{\mathbf{h}}_{\mathrm{B,L}}\right) - f\left(\widehat{\mathbf{h}}_{\mathrm{A,L}}\right) \tag{17}$$

where the function f satisfies $f\left(\mathbf{r}\right) = \mathbf{r}\left(\overline{\mathbf{R}}_1 \otimes \overline{\mathbf{R}}_{\mathrm{F}}\right)\mathbf{r}^{\mathrm{H}}$. The function f can be simplified by the following theorem:

Theorem 3. *When $N_{\mathrm{T}} \rightarrow \infty$, the error decision function can be simplified as:*

$$\Delta f = L\left\{\rho_1 - \mathrm{Tr}\left(\mathbf{R}_2\overline{\mathbf{R}}_1\right)\right\} \tag{18}$$

Proof: See proof in Appendix VII-D ∎

Examining this equation, we could find the pilot scheduling strategies of Ava across subcarriers do not affect the decision function. In what follows, we try to further acquire the characteristic of Δf from the observation of $\mathbf{R}_1$ and $\mathbf{R}_2$.

Algorithm 2 :Channel Estimation and Identification Enhancement

1: Identify whether attack happens through the codewords derived by using inner product in [6].
2: If attack happens, calculate the sample covariance matrix $\mathbf{C}_{\mathbf{Y}_{\mathrm{L}}} = \frac{1}{N_{\mathrm{T}}s}\mathbf{Y}_{\mathrm{L}}\mathbf{Y}_{\mathrm{L}}^{\mathrm{H}}$. Derive the two pilot signal vectors $\mathbf{x}_{\mathrm{L},1}$ and $\mathbf{x}_{\mathrm{L},2}$. Calculate the weight matrices and finally derive the FS channel estimations using Eq. (11). If no attack happens, just use LS estimator to get FS channels.
3: If no attack happens, directly derive CIR estimation using estimated FS channels, otherwise, calculate Δf using Eq. (17). According to Theorem 4, if $\Delta f > 0$, $\widehat{\mathbf{h}}_{\mathrm{B,L}}$ serves as the true estimated FS channel of Bob for further CIR estimating, otherwise $\Delta f < 0$, $\widehat{\mathbf{h}}_{\mathrm{A,L}}$ does. When $\Delta f = 0$, an identification error happens and the reliability breaks down.

---

1) Hints Derived from Spatial Correlation: The authors in [12] pointed out that the set of eigenvalues of $\mathbf{R}_i$ and the set of uniformly spaced samples $\left\{S_i\left(n/N_{\mathrm{T}}\right) : n = 0, \ldots, N_{\mathrm{T}} - 1\right\}$ are asymptotically equally distributed, i.e., for any continuous function $f\left(x\right)$. The function $S_i\left(x\right)$ over $x \in \left[-\frac{1}{2}, \frac{1}{2}\right]$ satisfies: $S_i\left(x\right) = \frac{1}{2\Delta}\sum\limits_{0\in\left[D\sin(\theta_i-\Delta)+x, D\sin(\theta_i+\Delta)+x\right]}\frac{1}{\sqrt{D^2-x^2}}$. And the channel covariance eigenvectors $\mathbf{U}_i$, i.e., $N_{\mathrm{T}} \times \rho_i$ matrix $\overline{\mathbf{U}}_i$, can be approximated with a submatrix of the DFT matrix $\mathbf{F}$ in the following sense: $\lim\limits_{N_{\mathrm{T}}\rightarrow\infty}\frac{1}{N_{\mathrm{T}}}\left\|\overline{\mathbf{U}}_i\overline{\mathbf{U}}_i^{\mathrm{H}} - \mathbf{F}_{\mathcal{S}_i}\mathbf{F}_{\mathcal{S}_i}^{\mathrm{H}}\right\|_{\mathrm{F}}^2 = 0, i = 1, 2$ where $\mathbf{F}_{\mathcal{S}_i} = \left(\mathbf{f}_n : n \in \mathcal{J}_{\mathcal{S}_i}\right)$ with $\mathcal{J}_{\mathcal{S}_i} = \left\{n, \left[n/N_{\mathrm{T}}\right] \in \mathcal{S}_i, n = 0, \ldots, N_{\mathrm{T}} - 1\right\}$ Here, $\mathcal{S}_i$ denotes the support of $S_i\left(x\right)$. Backing to the Eq. (18), the trace function satisfies $\mathrm{Tr}\left(\mathbf{R}_2\overline{\mathbf{R}}_1\right) \leq \mathrm{Tr}\left(\mathbf{\Lambda}_2\mathbf{U}_2^{\mathrm{H}}\mathbf{U}_1\overline{\mathbf{\Lambda}}_1\right) = \mathrm{Tr}\left(\mathbf{\Lambda}_{2,\mathrm{p}}\overline{\mathbf{U}}_2^{\mathrm{H}}\overline{\mathbf{U}}_1\overline{\mathbf{\Lambda}}_{1,\mathrm{p}}\right)$ where $\mathbf{\Lambda}_{i,\mathrm{p}}$ and $\overline{\mathbf{\Lambda}}_{i,\mathrm{p}}$ are respectively defined by $\mathbf{\Lambda}_{i,\mathrm{p}} = diag\left\{\begin{array}{ccc} \lambda_{i,1} & \cdots & \lambda_{i,\rho_i} \end{array}\right\}$ and $\overline{\mathbf{\Lambda}}_{i,\mathrm{p}} = diag\left\{\begin{array}{ccc} \lambda_{i,1}^{-1} & \cdots & \lambda_{i,\rho_i}^{-1} \end{array}\right\}$. As previously discussed, we approximate $\overline{\mathbf{U}}_2^{\mathrm{H}}\overline{\mathbf{U}}_1$ using $\mathbf{F}_{\mathcal{S}_2}^{\mathrm{H}}\mathbf{F}_{\mathcal{S}_1}$ and define $\mathcal{S}_1 \cap \mathcal{S}_2 = \mathcal{S}_3$. We then discuss the influence of $\mathcal{S}_3$ on $\mathrm{Tr}\left(\mathbf{\Lambda}_{2,\mathrm{p}}\overline{\mathbf{U}}_2^{\mathrm{H}}\overline{\mathbf{U}}_1\overline{\mathbf{\Lambda}}_{1,\mathrm{p}}\right)$. When $\mathcal{S}_3 = \emptyset$, we can have $\mathrm{Tr}\left(\mathbf{R}_2\overline{\mathbf{R}}_1\right) = 0$. When $\mathcal{S}_3 \neq \emptyset$, we assume $\mathcal{S}_3 = \mathcal{P}_a$ and have

$$\mathrm{Tr}\left(\mathbf{\Lambda}_{2,\mathrm{p}}\overline{\mathbf{U}}_2^{\mathrm{H}}\overline{\mathbf{U}}_1\overline{\mathbf{\Lambda}}_{1,\mathrm{p}}\right) \leq \sum_{j=1}^{a}\frac{\lambda_{2,i_j}}{\lambda_{1,i_j}} \tag{19}$$

This is because the eigenvectors labeled by the indexes out of the interacted set $\mathcal{S}_3$ are mutually orthogonal [12]. Then we have the following theorem:

Theorem 4. *When $N_{\mathrm{T}} \rightarrow \infty$, there always exists $\sum\limits_{j=1}^{a}\frac{\lambda_{2,i_j}}{\lambda_{1,i_j}} = a$. If $\theta_1 \neq \theta_2$, there must exist $a < \rho_1$ and $\Delta f > 0$. Otherwise if $\theta_1 = \theta_2$, there must exist $a = \rho_1$ and $\Delta f = 0$.*

Proof: See proof in Appendix VII-E ∎

2) IEP Reduction: Inspired by the above result, we know that the identification error happens only when $\theta_1 = \theta_2$.

Theorem 5. *Under the assumption of mean AoA obeying*

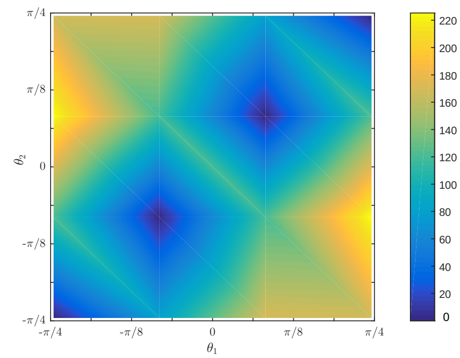

Fig. 3. Strength of Δf versus $\theta_i, i = 1, 2$ with $N_{\mathrm{T}} = 100$.

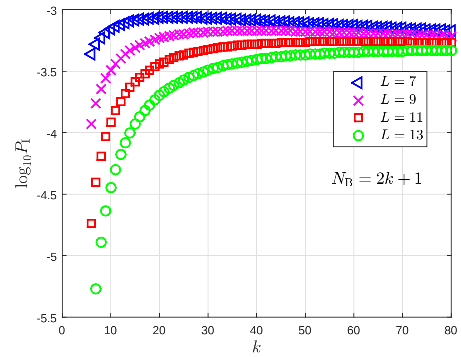

Fig. 4. Performance of IEP versus N_{B} under different L.

continuous probability distribution (CPD), the IEP P_{I} in Eq. (9) is updated to be zero. Under the assumption of mean AoA obeying distrete probability distribution (DPD), for instance, uniform distribution with interval length K, the IEP P_{I} in Eq. (9) is updated to be $\frac{P_{\mathrm{I}}}{K}$.

The proof is institutive. Therefore, the IEP can be seriously reduced and reliability is thus significantly enhanced under hybrid attack environment. Finally, we give the overall process of channel estimation and identification enhancement in Algorithm 2.

V. Numerical Results

In this section, we further carry out the performance evaluation concerning above techniques mentioned.

In this part, we aim to verify the feasibility of Theorem 4 through simulations shown in Fig. 3 where the strength of Δf is plotted against $\theta_i, i = 1, 2$ by configuring $N_{\mathrm{T}} = 100$ and $K = 5$. In this simulation, we consider that the candidate samples of discrete mean AoAs lie within the set $\left\{-\frac{\pi}{4}, -\frac{\pi}{7}, 0, -\frac{\pi}{7}, -\frac{\pi}{4}\right\}$. Based on the estimation in Eq. (11) and the correlation model in Eq. (4), we derive the corresponding examples of Δf. As we can see, the identification error happens when $\Delta f = 0$, that is, $\theta_1 = \theta_2$. In this sense, we could envision that the IEP is zero under the assumption of the mean AoA with CPD.

For the sake of a comprehensive analysis, we consider the DPD model for mean AoA and further simulate the IEP performance in Fig. 4. The mean AoA is discretely and uniformly distributed in a length-K interval. As shown in this figure, the performance of IEP is plotted versus the length of N_{B} under different number L of channel taps. We consider L to be from 7 to 13 and K to be 20. k, related to N_{B}, satisfies $N_{\mathrm{B}} = 2k + 1$. As we can see, even with small subcarrier overheads, that is, N_{B} is small, the IEP can be low and our architecture has a very reliable performance guarantee. Moreover, we can find that when L is low, such as $L = 7$, the IEP has a maximum value after which IEP decreases with the increase of N_{B}. With the increase of L, IEP decreases monotonically with N_{B}. Furthermore, the initial value of L determines the upper bound IEP can achieve. With the increase of L, the upper bound decreases. For instance, the upper bound of P_{I} achieves as low as $10^{-3.3}$ at $k = 80$ when L is equal to 9. In this case, the number of occupied subcarriers satisfies $N_{\mathrm{B}} = 161$.

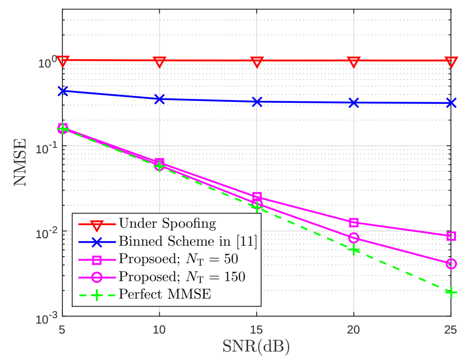

Fig. 5. NMSE of CIR estimation versus SNR under different number of antennas.

Finally, we simulate the performance of channel estimation in Fig. 5 in which the NMSE is plotted versus SNR of Bob under different number of antennas. L and N_{B} are respectively configured to be 6 and 256. Here, we consider the estimation shown in Eq. (11) and assume perfect identification for attacks. We do not consider the case where there is no attack since in this case LS estimator is a natural choice. For the simplicity of comparison, we only present the channel estimation under PTS attack because the estimation error floor under PTN and PTJ attack can be easily understood to be very high. The binned scheme proosed in [11] is simulated as an another comparison scheme. As we can see, PTS attack, if happens, causes a high-NMSE floor on CIR estimation for Bob. This phenomenon can also be seen in the binned scheme. However, the estimation in our proposed framework breaks down this floor and its NMSE gradually decreases with the increase of transmitting antennas. Also, we consider perfect MMSE to be a performance benchmark for which perfect pilot tones, including Ava's pilot tones, are assumed to be known by Alice. We find that the NMSE brought in our scheme gradually approaches the level under perfect MMSE with the increase of antennas. That's because the estimator highly relies on the statistical property of $\mathbf{C}_{\mathbf{Y}_{\mathrm{L}}}$, determined by the number of antennas.

VI. Conclusions

This paper investigated the issue of pilot-aware attack on the uplink channel training process in large-scale MISO-OFDM systems. We proposed a secure ICCB uplink training architecture in which pilot tones, usually exposed in public, are now enabled to be shared between legitimate transceiver pair under hybrid attack environment. We developed a novel coding theory to support and secure this pilot sharing process, and found an optimal code rate to finally provide the well-imposed CIR estimation. Theoretically, we verified an important fact that this architecture could perfectly secure pilot sharing against the attack if the CPD model of mean AoA was considered. In practical scenarios with DPD model of mean AoA, this architecture could also bring a high-reliability and high-precision CIR estimation.

VII. Appendix

A. Proof of Theorem 1

Since codewords in this constant-weight code are constrained to be with same and fixed length, the number of overlapping digits achieves its minimum only when the zero digits of each codeword are fully occupied. In this case, the remanent digits, i.e., the overlapping digits, account for $2w - N_{\mathrm{B}}$ which should be equal to s and less than w. Therefore, we can prove the theorem.

B. Proof of Theorem 2

To guarantee well-imposed CIR estimation, there should be $s \geq L$, that is, $\mathbf{F}_{\mathrm{L},s}$ is with full column rank. However, the increase of s will reduce the code rate since the function of C decreases with s. Therefore, the optimal code rate is proved.

Considering the hybrid attack, we know that their exists the possibility of $2^{N_{\mathrm{B}}}$ codewords to appear. Two interpreted codewords derived by inner-product operation in [6], if satisfying the same weight constraint, will confuse Alice. In this case, each assumption is decided with the probability of 0.5. The possible number of codewords that satisfy this condition is equal to $\frac{N_{\mathrm{B}}!}{\left(\frac{N_{\mathrm{B}}+L}{2}\right)!\left(\frac{N_{\mathrm{B}}-L}{2}\right)!}$. One exception is when the codeword of Ava is identical to that of Bob. In this case, the codeword can be uniquely determined. Finally, there exists the possibility of $\frac{N_{\mathrm{B}}!}{\left(\frac{N_{\mathrm{B}}+L}{2}\right)!\left(\frac{N_{\mathrm{B}}-L}{2}\right)!} - 1$ codewords that could cause identification errors. Then the ultimate IEP can be proved.

C. Proof of Proposition 2

Take Bob for example, we can derive the error of MMSE based estimation as $\varepsilon_{\mathrm{B}}^2 = T\left(1 - T\mathbf{X}_{\mathrm{L},1}^{\mathrm{H}}\mathbf{C}_{\mathbf{Y}_{\mathrm{L}}}^{-1}\mathbf{X}_{\mathrm{L},1}\right)$.

$\mathbf{C}_{\mathbf{Y}_{\mathrm{L}}}$ is transformed into $\mathbf{C}_{\mathbf{Y}_{\mathrm{L}}} \xrightarrow[N_{\mathrm{T}}\to\infty]{\text{a.s.}} \frac{1}{N_{\mathrm{T}}s}\mathbf{X}_{\mathrm{L}}\mathbf{R}_{\mathrm{C}}\mathbf{X}_{\mathrm{L}}^{\mathrm{H}} + \sigma^2\mathbf{I}_2$ using asymptotic approximation [16]. Here, the 2×2 matrix $\mathbf{R}_{\mathrm{C}}$ satisfies $\mathbf{R}_{\mathrm{C}} = \mathrm{diag}\left\{ \mathrm{Tr}\left(\mathbf{R}_1\right)\mathrm{Tr}\left(\mathbf{R}_{\mathrm{F}}\right) \quad \mathrm{Tr}\left(\mathbf{R}_2\right)\mathrm{Tr}\left(\mathbf{R}_{\mathrm{F}}\right) \right\}$. Therefore, we can derive $\varepsilon_{\mathrm{B}}^2 = T\left\{1 - \mathbf{X}_{\mathrm{L},1}^{\mathrm{H}}\left(\mathbf{X}_{\mathrm{L}}\mathbf{X}_{\mathrm{L}}^{\mathrm{H}}\right)^{-1}\mathbf{X}_{\mathrm{L},1}\right\}$ at high SNR region. In the same way, we can derive $\varepsilon_{\mathrm{A}}^2 = T\left\{1 - \mathbf{X}_{\mathrm{L},2}^{\mathrm{H}}\left(\mathbf{X}_{\mathrm{L}}\mathbf{X}_{\mathrm{L}}^{\mathrm{H}}\right)^{-1}\mathbf{X}_{\mathrm{L},2}\right\}$. After calculating the matrix inverse and performing matrix multiplication, we can finally verify $\varepsilon_{\mathrm{B}}^2 = \varepsilon_{\mathrm{A}}^2$. This completes the proof.

D. Proof of Theorem 3

Thanks to $\widehat{\mathbf{h}}_{\mathrm{B,L}} = \mathbf{h}_{\mathrm{B,L}} - \varepsilon_{\mathrm{B}}\mathbf{h}$, $f\left(\widehat{\mathbf{h}}_{\mathrm{B,L}}\right)$ can be expressed as: $f\left(\widehat{\mathbf{h}}_{\mathrm{B,L}}\right) = \left(\mathbf{h}_{\mathrm{B,L}} - \varepsilon_{\mathrm{B}}\mathbf{h}\right)\left(\overline{\mathbf{R}}_1 \otimes \overline{\mathbf{R}}_{\mathrm{F}}\right)\left(\mathbf{h}_{\mathrm{B,L}} - \varepsilon_{\mathrm{B}}\mathbf{h}\right)^{\mathrm{H}}$ then this equation can be expanded into $f\left(\widehat{\mathbf{h}}_{\mathrm{B,L}}\right) = f_1 - 2f_2 + f_3$ where $f_1 = \mathbf{h}_{\mathrm{B,L}}\left(\overline{\mathbf{R}}_1 \otimes \overline{\mathbf{R}}_{\mathrm{F}}\right)\mathbf{h}_{\mathrm{B,L}}^{\mathrm{H}}$ and $f_2 = \varepsilon_{\mathrm{B}}\mathbf{h}_{\mathrm{B,L}}\left(\overline{\mathbf{R}}_1 \otimes \overline{\mathbf{R}}_{\mathrm{F}}\right)\mathbf{h}$, $f_3 = \varepsilon_{\mathrm{B}}^2\mathbf{h}\left(\overline{\mathbf{R}}_1 \otimes \overline{\mathbf{R}}_{\mathrm{F}}\right)\mathbf{h}$. By using the asymptotic approximation for each term, we can have $f\left(\widehat{\mathbf{h}}_{\mathrm{B,L}}\right) \xrightarrow[N_{\mathrm{T}}\to\infty]{\text{a.s.}} \rho_1 L + \varepsilon_{\mathrm{B}}^2\mathrm{Tr}\left(\overline{\mathbf{R}}_1 \otimes \overline{\mathbf{R}}_{\mathrm{F}}\right)$ In the same way, we can simplify the function $f\left(\widehat{\mathbf{h}}_{\mathrm{A,L}}\right)$ as: $f\left(\widehat{\mathbf{h}}_{\mathrm{A,L}}\right) \xrightarrow[N_{\mathrm{T}}\to\infty]{\text{a.s.}} L\mathrm{Tr}\left(\mathbf{R}_2\overline{\mathbf{R}}_1\right) + \varepsilon_{\mathrm{A}}^2\mathrm{Tr}\left(\overline{\mathbf{R}}_1 \otimes \overline{\mathbf{R}}_{\mathrm{F}}\right)$ As indicated in Proposition 2, there exists $\varepsilon_{\mathrm{B}}^2 = \varepsilon_{\mathrm{A}}^2$. By comparing $f\left(\widehat{\mathbf{h}}_{\mathrm{B,L}}\right)$ and $f\left(\widehat{\mathbf{h}}_{\mathrm{A,L}}\right)$, we can complete the proof.

E. Proof of Theorem 4

First, we will prove $\sum_{j=1}^{a}\frac{\lambda_{2,i_j}}{\lambda_{1,i_j}} = a$. As shown in [12], the empirical CDF of eigenvalues of $\mathbf{R}_i$ can be asymptotically approximated using the collection of samples from $\left\{S_i\left([n/N_{\mathrm{T}}]\right), n = 0, \ldots, N_{\mathrm{T}} - 1\right\}$. Therefore, the eigenvalues of different individuals, if overlapping at the same location n, can be approximated with the same eigenvalues.

Then we prove that there must $a < \rho_1$. Examining $[\theta_2 - \Delta, \theta_2 + \Delta]$ and $[\theta_1 - \Delta, \theta_2 + \Delta]$ we found if $\theta_1 \neq \theta_2$ is satisfied, there must exist $a < \rho_1$ since $[\theta_2 - \Delta, \theta_2 + \Delta]$ must have non-empty intersection with $[\theta_1 - \Delta, \theta_1 + \Delta]$. In this case, the number of elements in $\mathcal{S}_3$ is reduced to be smaller than that ρ_1. Now we turn to the case $\theta_1 = \theta_2$ in which we easily have $\mathbf{R}_1 = \mathbf{R}_2$ and therefore the theorem is proved.

References

[1] T. Bogale and L. B. Le, “Massive MIMO and mmWave for 5G wireless HetNet: Potentials and challenges,” *IEEE Veh. Technol. Mag.*, vol. 11, no. 1, pp. 64-75, Feb. 2016.

[2] C. Shahriar, M. La Pan, M. Lichtman, T. C. Clancy, R. McGwier, R. Tandon, S. Sodagari, and J. H. Reed, “PHY-Layer resiliency in OFDM communications: A tutorial,” *IEEE Commun. Surveys Tuts.*, vol. 17, no. 1, pp. 292-314, Aug. 2015.

[3] H. Pirzadeh, S. M. Razavizadeh, and E. Bjornson, “Subverting massive MIMO by smart jamming,” *IEEE Wireless Commun. Lett.*, vol. 5, no. 1, pp. 20-23, Feb. 2016.

[4] M. Ozdemir and H. Arslan, “Channel estimation for wireless OFDM systems,” *IEEE Commun. Surveys Tuts.*, vol. 9, no. 2, pp. 18-48, 2nd Quart. 2007.

[5] T. C. Clancy, “Efficient OFDM denial: Pilot jamming and pilot nulling,” in *Proc. IEEE Int. Conf. Commun.*, June 2011, pp. 1-5.

[6] D. Xu, P. Ren, Y. Wang, Q. Du, and L. Sun, “ICA-SBDC: a channel estimation and identification mechanism for MISO-OFDM systems under pilot spoofing attack,” in *Proc. IEEE Int. Conf. Commun. (ICC)*, May 2017, pp. 1-5.

[7] X. Zhou, B. Maham, and A. Hjorungnes, “Pilot contamination for active eavesdropping,” *IEEE Trans. Wireless Commun.*, vol. 11, no. 3, pp. 903-907, Mar. 2012.

[8] D. Kapetanovic, G. Zheng, K.-K. Wong, and B. Ottersten, “Detection of pilot contamination attack using random training and massive MIMO,” in *Proc. IEEE Int. Symp. on Personal, Indoor and Mobile Radio Commun. (PIMRC'13)*, Sep. 2013, pp. 13-18.

[9] J. K.Tugnait, “Self-contamination for detection of pilot contamination attack in multiple antenna systems,” *IEEE Wireless Commun. Letters*, vol. 4, no. 5, pp. 525-528, Oct. 2015.

[10] D. Kapetanovic, A. Al-Nahari, A. Stojanovic, and F. Rusek, “Detection of active eavesdroppers in massive MIMO,” in *Proc. IEEE Int. Symp. on Personal Indoor and Mobile Radio Commun. (PIMRC’14)*, Sep. 2014, pp. 585-589.

[11] C. Shahriar and T. C. Clancy, “Performance impact of pilot tone randomization to mitigate OFDM jamming attacks,” in *Proc. IEEE CCNC*, Jan. 2013, pp. 813-816.

[12] A. Adhikary, J. Nam, J.-Y. Ahn, and G. Caire, “Joint spatial division and multiplexing-The large-scale array regime,,” *IEEE Trans. Inf. Theory*, vol. 59, no. 10, pp. 6441-6463, Oct. 2013.

[13] B. Han and Y. R. Zheng, “Higher rank principal Kronecker model for triply selective fading channels with experimental validation,” *IEEE Trans. Veh. Technol.*, vol. 64, no. 5, pp. 1654-1663, May 2015.

[14] M. R. McKay, P. J. Smith, H. A. Suraweera, and I. B. Collings, “On the mutual information distribution of OFDM-based spatial multiplexing: exact variance and outage approximation,” *IEEE Trans. Inf. Theory*, vol. 54, no. 7, pp. 3260-3278, 2008.

[15] M. Z. Shakir, A. Rao, and M.-S. Alouini, “On the decision threshold of eigenvalue ratio detector based on moments of joint and marginal distributions of extreme eigenvalues,” *IEEE Trans. Wireless Commun.*, vol. 12, no. 3, pp. 974-983, Mar. 2013.

[16] J. Hoydis, S. ten Brink, and M. Debbah, “Massive MIMO in the UL/DL of cellular networks: How many antennas do we need?” *IEEE J. Sel. Areas Commun.*, vol. 31, no. 2, pp. 160-171, Feb. 2013.